




Beam Scanning Realized by Coupled Modes in a Single-Patch Antenna

Haozhan Tian , *Student Member, IEEE*, Kirti Dhawaj , *Student Member, IEEE*,
Li Jun Jiang, *Senior Member, IEEE*, and Tatsuo Itoh , *Life Fellow, IEEE*

Abstract—In this letter, we introduce a novel beam scanning in a single-rectangular-patch antenna realized by coupled modes. The design exhibits radiated beams that scan as a function of frequency, but is different in its operation mechanism compared to a traditional leaky-wave antenna. The idea is to manipulate the phase difference between the fields at two radiating slots of the antenna to reform the beam. Metal vias are introduced to create two coupled half-mode cavities in the patch antenna. The mutual coupling between the two cavities makes the phase difference as a function of the operating frequency. The simulated beam scans from broadside to 43° within the 3 dB gain band. The implemented sample realizes 4.55% bandwidth of S_{11} with center frequency at 5.05 GHz by measurement. The beam scans from 14° to 34° within the matching band, which is confirmed by both simulation and measurement. The measured radiation efficiency within the matching band is comparable to a regular-patch antenna.

Index Terms—Beam steering, filtering theory, mutual coupling, patch antenna, phased array.

I. INTRODUCTION

RECTANGULAR patch antenna has been widely used in many applications due to its simplicity and low cost as well as the compact configuration [1]. The fundamental mode of operation for this antenna is TM_{100}^z , which offers the maximum electric fields with 180° phase difference at two radiating slots. The radiation mechanism of the patch antenna has been typically explained from two perspectives. In the transmission-line model, the radiation is from in-phase fringing fields at two radiation slots. In the cavity model, it is from two in-phase equivalent magnetic currents. Derived from either of the explanations, the radiation pattern of the patch antenna is basically independent on the frequency as long as the operation mode remains the same.

Beam-scanning antennas, on the other hand, are desired for many applications. A good example is the leaky-wave antenna whose beam pattern scans in the space as the operating frequency changes [2]. The radiation for this type of antenna is realized by leaking energy gradually as the wave propagates

along the structure. The beam-scanning angle is then dictated by the frequency-dependent propagation constant [3]. In order to maintain a high radiation efficiency, the antenna has to be longer than wavelength in general. Another way is to use the phased array [4]. The beam scanning can be realized by properly tuning the phase and amplitude of each element. However, the structure of an array can be bulky and complex.

In this letter, we introduce coupled modes in a patch antenna to realize beam scanning. The phase difference of two radiation slots can be manipulated by our design. The beam scans from broadside to 43° within 3 dB realized boresight gain bandwidth in simulation. The implemented sample realizes 4.55% 10 dB bandwidth of S_{11} with center frequency at 5.05 GHz by measurement. The design shares the simple and compact configuration of patch antenna while maintaining a high radiation efficiency in the meantime. The operation mechanism along with the results of simulation and measurement are presented in the following sections.

II. BEAM SCANNING USING MUTUAL COUPLING

Shown in Fig. 1 is the schematic of the proposed antenna. A ground-backed Rogers RT/Duroid 5880 substrate is used for the design, with dielectric constant of 2.2, loss tangent of 0.001, and height of 0.79 mm. The antenna is based on a typical rectangular patch antenna with an inset feedline. The size of the antenna is characterized by the width w and total length $l_{\text{total}} = 2l + \Delta l$. We introduce metal vias around the center connecting the patch with the ground. These metal vias behave like a metal wall for the electromagnetic field in the substrate, which divide the patch cavity into two parts. Each part is a resonator, which supports a half-mode of TM_{100} , such as the mode in a planar inverted-F antenna [5]. A gap with the width of $s = 3.5$ mm is opened on the interior wall by removing some metal vias. It functions as a coupling iris.

A. Operation

The mutual coupling between two cavities results in two eigenmode solutions, which are called even mode, due to electric coupling, and odd mode, due to magnetic coupling. For simplicity, let us first analyze a symmetric structure, as shown in Fig. 2, where the dashed line is at the center and thus the two half-mode cavities are identical. The E-field distributions of even and odd modes are demonstrated in Fig. 2(a) and (b), respectively. The structure can then be modeled by an array of

Manuscript received March 19, 2018; revised April 16, 2018; accepted April 28, 2018. Date of publication May 2, 2018; date of current version June 4, 2018.
(Corresponding author: Haozhan Tian.)

H. Tian, K. Dhawaj, and T. Itoh are with the Department of Electrical and Computer Engineering, University of California, Los Angeles, CA 90095 USA (e-mail: haozhan@ucla.edu; kdhawaj@gmail.com; itoh@ee.ucla.edu).

L. J. Jiang is with the Department of Electrical and Electronics Engineering, University of Hong Kong, Hong Kong (e-mail: jianglj@hku.hk).

Digital Object Identifier 10.1109/LAWP.2018.2832605

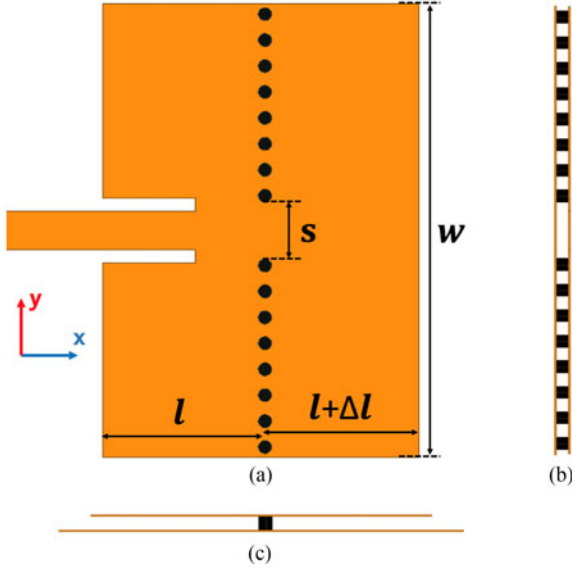


Fig. 1. Schematic of the proposed design. (a) Top view. The black dots are the metal via connecting top metal to the ground. The dimensions are all in millimeters: $l = 9.5$, $\Delta l = 0.5$, $w = 28$, $s = 3.5$. The height of the board is $h = 0.79$ mm. The diameter of the via is 0.8 mm and the spacing is 1.6 mm. (b) Side view. (c) Front view.

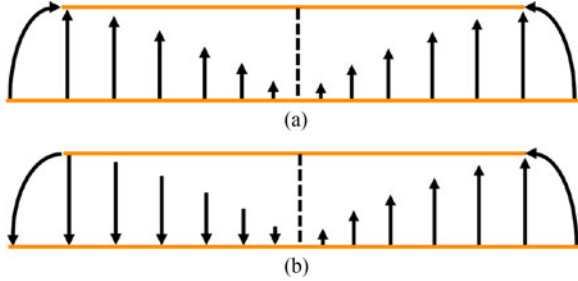


Fig. 2. Demonstration of coupled E-field distribution in symmetric structure at (a) even mode and (b) odd mode. The dashed line represents the via wall with an open gap for coupling.

two equivalent magnetic currents with the same amplitude but different phases. In the xz plane, the array factor (AF) is given by [1]

$$AF = 2 \cos \left[\frac{1}{2} (k_0 d \sin \theta + \Delta \phi) \right] \quad (1)$$

where k_0 is the propagation constant in free space, d is the separation distance, and $\Delta \phi$ is the phase difference of the two magnetic currents. The pattern of one of the magnetic currents on the E -plane is approximately omnidirectional, and thus, beam pattern of the array on the E -plane is only dependent on AF. In the even-mode case where $\Delta \phi = 180^\circ$, there will be a null at broadside $\theta = 0^\circ$ in the far-field pattern due to the out-of-phase cancellation. Meanwhile for the odd mode where $\Delta \phi = 0^\circ$, the structure will radiate like a rectangular patch antenna where the beam peak is at the broadside. As frequencies change from even mode to odd mode, the phase difference $\Delta \phi$ will gradually shift from 0° to 180° due to the coupling. In consequence, the beam peak will scan away from broadside according to (1).

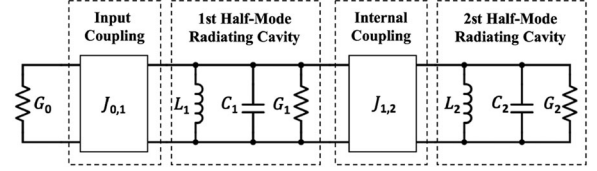


Fig. 3. Equivalent lumped circuit model where radiation loss of the two cavities is represented by G_1 and G_2 , respectively. Parameters: $G_0 = 0.02$ S, $J_{0,1} = 1.035 \times 10^{-2}$ S, $L_1 = 0.278$ nH, $C_1 = 3.575$ pF, $G_1 = 4.040 \times 10^{-3}$ S, $J_{1,2} = 3.938 \times 10^{-3}$ S, $L_2 = 0.264$ nH, $C_2 = 3.771$ pF, $G_2 = 3.856 \times 10^{-3}$ S.

However, far-field cancellation and two equal lobes in the radiation pattern of even mode are undesired since one main beam scanning around the broadside is our goal. Thus, we introduce asymmetry to the model by putting the vias slightly off the center so that the two cavities are not identical. In this way, the fields coupling at the iris will pass through different electrical lengths to reach the two radiating edges, respectively. So the phase difference at even mode is close to 180° but not exactly at 180° , which avoids the strong broadside cancellation, and leads to one main beam instead of two equal lobes at even mode. In the meantime, the beam peak also shifts slightly away from the broadside at odd mode due to the asymmetry. The even mode or odd mode is defined by the type of coupling that happens at the iris, not by the phase difference between the two radiation slots. That means the even and odd modes are still two eigenmode solutions of an asymmetric model. It has to be mentioned that there will still be a minor lobe and a null in the radiation pattern scanning with frequency as predicted by (1). In fact, we may benefit from the scanning null, as reported in [6], in some applications such as cognitive radio. We will leave this discussion for the future.

B. Design From a Filtering Antenna Perspective

The design philosophy is borrowed from the procedure to design a filtering antenna [7]. The idea is first to generate a circuit model to meet the desired operation frequency and the bandwidth, as the design procedures of a two-pole passband filter. In this way, we can determine how fast the beam scans with frequency and get reasonable realized boresight gain within the band. Unlike traditional two-port filter, the model of our design is built with only source port but no load port. This is because the energy from the input source of this design will be radiated out directly to the free space instead of a load port as the traditional two-port passband filter. However, load is still necessary, so in our model, the radiation conductance of the antenna is regarded as equivalent load.

In Fig. 3, the equivalent lumped circuit model is built for a fractional bandwidth of 4.8% at the midband frequency 5.05 GHz. The shunt LC circuits represent the resonance of the two half-mode cavities. G_1 and G_2 stand for the equivalent radiation conductances, which can be theoretically calculated by [1]

$$G_i = \frac{W}{120\lambda_i} \left[1 - \frac{1}{24} \left(\frac{2\pi h}{\lambda_i} \right)^2 \right] \quad (2)$$

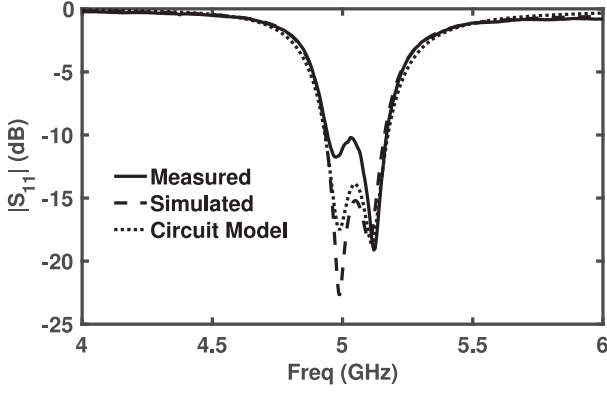


Fig. 4. Simulated, measured, and circuit-model S_{11} response.

where λ_i is the resonant wavelength in each cavity, for $i = 1, 2$. The interstage couplings are modeled by the admittance inverters, whose values are related to external quality factor Q_e and coupling coefficient k by

$$Q_e = \frac{b_1 G_0}{J_{0,1}^2} \quad (3)$$

$$k = \frac{J_{1,2}}{\sqrt{b_1 b_2}} \quad (4)$$

where $b_i = 2\pi f_i C_i$ for $i = 1, 2$. By applying the methods of filter designs in [8], the parameter values of the model can be calculated. The response of the circuit model is shown in Fig. 4 to compare with the one of simulation and measurement.

The structure of the antenna can be designed based on the values of the circuit model. The dimensions of the two half-mode cavities are calculated following similar procedures for designing rectangular patches [1]. It has to be mentioned that besides the fields of cavity mode, the fringing fields at the radiation slots contribute to the shunt LC circuits in the circuit model as well. The inset feed is designed to guarantee a desired external coupling as indicated in (3), which leads to a good input matching. The gap size is determined by the internal coupling coefficient extracted from the circuit model by (4). With minor optimization to compensate the inaccuracy of the approximations, the final structure is then designed as shown in Fig. 1.

III. SIMULATION AND MEASUREMENT

The simulated, measured, and circuit-model S_{11} responses match well with each other, as shown in Fig. 4. The reflection coefficient of the antenna is measured by Agilent 8510C vector network analyzer. The measured center frequency is 5.05 GHz with 10 dB fractional bandwidth of 4.55%. The measured fractional bandwidth is slightly reduced from the desired 4.8% due to the fabrication errors. The two poles in the measured response are at 4.975 and 5.12 GHz, whereas the intermediate frequency peak is at 5.03 GHz.

In Fig. 5, the vector distribution of the E-field at these three frequencies are shown. The fields at 4.975 and 5.12 GHz represent the even- and odd-mode field distributions, respectively. The distributions are apparently asymmetric because the two

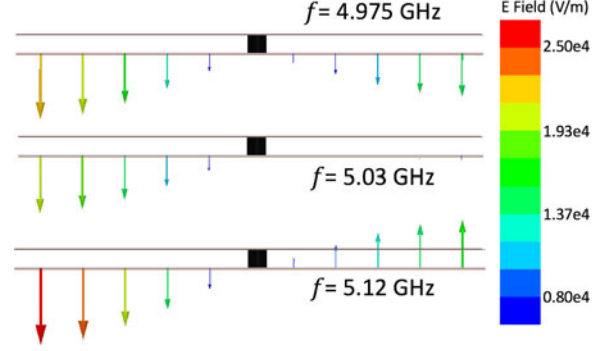


Fig. 5. Simulated vector distribution of the electric field in the substrate on the cross section. Three frequencies refer to even mode, the mode at the intermediate peak frequency, and odd mode.

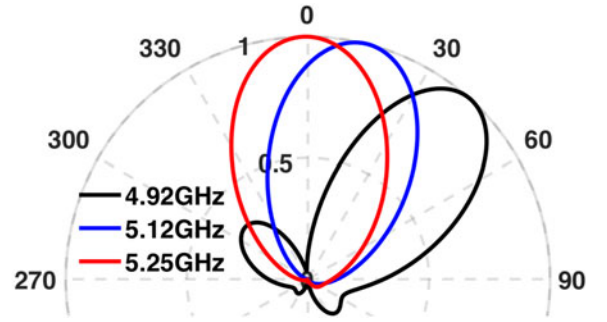


Fig. 6. Simulated copolarized radiation patterns on the E -plane. The patterns are normalized to 1 and shown in absolute value.

cavities are designed to be nonidentical. This is desired for the radiation purpose as mentioned earlier. At 5.03 GHz, the fields at the two edges are around 90° out of phase. The field distributions for these three frequencies strongly support our theory that the phase difference at the two radiating slots changes with the operating frequency.

To demonstrate the beam-steering capability of our design, we plot the simulated radiation patterns on the E -plane at three selected frequencies, as shown in Fig. 6. The odd-mode frequency of 5.12 GHz is the frequency where maximum realized gain of 8.12 dBi is achieved in simulation. While at 4.92 and 5.25 GHz, the realized boresight gain is 3 dB lower than the maximum one, as shown in Fig. 7. The beam peak is at the broadside at 5.25 GHz, and it is at 43° at 4.92 GHz, which indicates a maximum 43° of scanning range within 3 dB gain band. The patterns are normalized to 1 and plotted in absolute values to provide a clear view of the beam steering.

The measured and simulated patterns on the E -plane compare closely for even-mode, 90-out-of-phase, and odd-mode frequencies, as shown in Fig. 8. The peak of the copolarized beam clearly scans from side to the center as the frequency changes. There is a -25 dB null at 341° on the copolarized pattern at 4.975 GHz. This is the cancellation for the even-mode radiation as discussed previously. The null scans to 324° as the frequency tuning to 5.03 GHz and disappears at 5.12 GHz. The measured cross-polarized patterns on the E -plane are all below

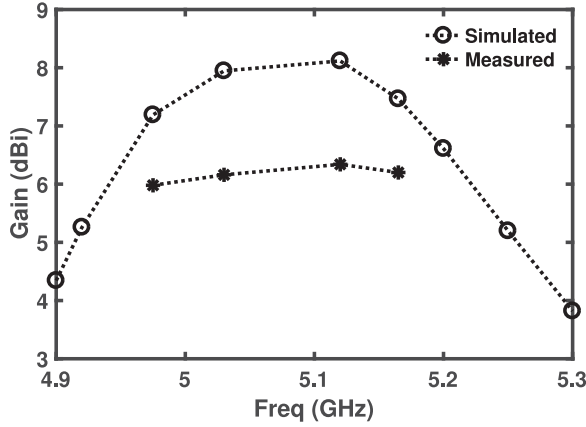


Fig. 7. Realized boresight gain versus frequency. The measured gains are at 4.975, 5.03, 5.12, and 5.165 GHz, respectively.

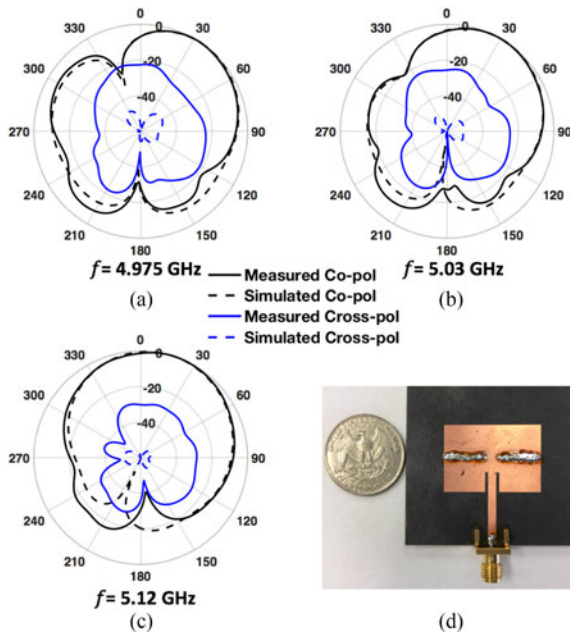


Fig. 8. Simulated and measured radiation patterns on the E -plane at (a) 4.975 GHz (even mode), (b) 5.03 GHz (90° out of phase), and (c) 5.12 GHz (odd mode). The implementation of the design is shown in (d).

−20 dB, though they are higher than the simulated ones due to fabrication and measurement tolerances.

The realized gain patterns at different frequencies on the E -plane are measured and shown in Fig. 9. The beam scans from 14° to 34° as the frequency changes from 5.165 to 4.975 GHz. The maximum realized gain of 6.34 dBi is achieved at 5.12 GHz, the odd-mode frequency, as predicted by simulation. At even-mode frequency 4.975 GHz, the realized gain is 5.98 dBi with radiation efficiency of 70.1%. Radiation efficiency mentioned in this letter is the ratio of radiated power to input power, which does not account for reflection loss due to mismatch. The highest radiation efficiency within the matching band is 73.8% realized

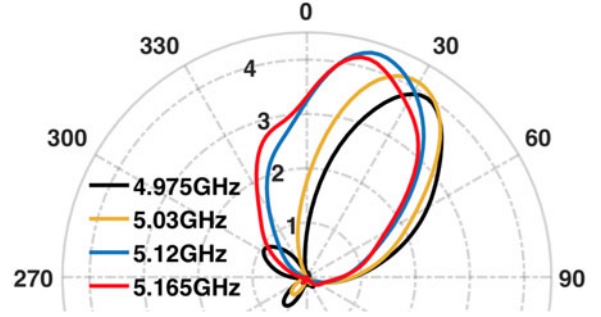


Fig. 9. Measured realized gain patterns in absolute value on the E -plane.

at 5.165 GHz, where the realized gain of 6.2 dBi is slightly lower than the maximum due to reflection loss.

As a comparison, a patch antenna, which has exactly the same configuration as the proposed design but has no vias, is fabricated and measured. It matches at 5.03 GHz with 1.4% matching bandwidth. The measured realized gain is 6.85 dBi, and radiation efficiency is 78.2% at 5.03 GHz. In comparison to the regular-patch antenna, the proposed antenna realizes the beam steering within a much wider matching bandwidth and maintains similar radiation efficiency in the same time.

IV. CONCLUSION

A novel beam scanning in a single-patch antenna is presented. The design is implemented by putting vias to create two coupled half-mode cavities in a rectangular patch antenna. We are able to manipulate the phase difference between the two equivalent magnetic currents and thus steer the beam through this design. Circuit model is built in order to control the coupling and achieve the wide matching bandwidth. Measured and simulated results show that the beam scans over a large range as the frequency changes while maintaining high radiation efficiency. The proposed beam-scanning antenna has advantages of compact size and low cost. It can be easily scaled to high-frequency domain due to the simplicity. The idea of phase manipulation within a single patch can potentially benefit many patch array designs.

REFERENCES

- [1] C. A. Balanis, *Antenna Theory: Analysis and Design*, 3rd ed., Hoboken, NJ, USA: Wiley, 2005.
- [2] L. Liu, C. Caloz, and T. Itoh, "Dominant mode leaky-wave antenna with backfire-to-endfire scanning capability," *Electron. Lett.*, vol. 38, no. 23, pp. 1414–1416, 2002.
- [3] D. R. Jackson, C. Caloz, and T. Itoh, "Leaky-wave antennas," *Proc. IEEE*, vol. 100, no. 7, pp. 2194–2206, Jul. 2012.
- [4] A. K. Bhattacharyya, *Phased Array Antennas: Floquet Analysis, Synthesis, BFNs and Active Array Systems*, vol. 179. Hoboken, NJ, USA: Wiley, 2006.
- [5] R. Vaughan, "Model and results for single mode PIFA antenna," in *Proc. IEEE Antennas Propag. Soc. Int. Symp.*, 2004, vol. 4, pp. 4028–4031.
- [6] X. Jiang, Z. Zhang, Y. Li, and Z. Feng, "A novel null scanning antenna using even and odd modes of a shorted patch," *IEEE Trans. Antennas Propag.*, vol. 62, no. 4, pp. 1903–1909, Apr. 2014.
- [7] Y. Yusuf and X. Gong, "Compact low-loss integration of high- q 3-d filters with highly efficient antennas," *IEEE Trans. Microw. Theory Techn.*, vol. 59, no. 4, pp. 857–865, Apr. 2011.
- [8] J. S. G. Hong and M. J. Lancaster, *Microstrip Filters for RF/Microwave Applications*, 2nd ed. Hoboken, NJ, USA: Wiley, 2011.